Exercise alleviates neovascular age-related macular degeneration by inhibiting AIM2 inflammasome in myeloid cells

Metabolism 144 (2023) 155584

Contents lists available at ScienceDirect

Metabolism

journal homepage: www.journals.elsevier.com/metabolism

Exercise alleviates neovascular age-related macular degeneration by inhibiting AIM2 inflammasome in myeloid cells

Bohao Cui [a], Xu Guo [a,1], Wei Zhou [a,1], Xiaodan Zhang [a,1], Kai He [a], Tinghui Bai [a], Dongxue Lin [a], Selena Wei-Zhang [a], Yan Zhao [b], Shengnan Liu [a], Hui Zhou [a], Qing Wang [c], Xueming Yao [a], Ying Shi [b], Ruotian Xie [a,b], Xue Dong [a,b], Yi Lei [a], Mei Du [a,b], Yongsheng Chang [d], Heping Xu [e], Dongming Zhou [f], Ying Yu [b], Xiaohong Wang [a,b,*], Hua Yan [a,g,**]

[a] Department of Ophthalmology, Tianjin Medical University General Hospital, Laboratory of Molecular Ophthalmology, Tianjin Key Laboratory of Ocular Trauma, Tianjin Medical University, Tianjin, China
[b] Department of Pharmacology, Tianjin Key Laboratory of Inflammation Biology, The Province and Ministry Co-sponsored Collaborative Innovation Center for Medical Epigenetics, School of Basic Medical Sciences, Tianjin Medical University, Tianjin, China
[c] Department of Clinical Laboratory, Tianjin Medical University General Hospital, Tianjin, China
[d] Department of Physiology and Pathophysiology, School of Basic Medical Sciences, Tianjin Medical University, Tianjin, China
[e] The Wellcome-Wolfson Institute for Experimental Medicine, Queen's University Belfast, 97 Lisburn Road, Belfast BT9 7BL, UK
[f] Department of Pathogen Biology, School of Basic Medical Sciences, Tianjin Medical University, Tianjin, China
[g] School of Medicine, Nankai University, 300071 Tianjin, China

ARTICLE INFO

Keywords:
Age-related macular degeneration
Anti-angiogenic therapy
Exercise
Adiponectin
AIM2 inflammasome

ABSTRACT

The neovascular form of age-related macular degeneration (nvAMD) is the leading cause of blindness in the elderly population. Vascular endothelial growth factor (VEGF) plays a crucial role in choroidal neovascularization (CNV), and anti-VEGF therapy is recommended as first-line therapy for nvAMD. However, many patients do not radically benefit from this therapy. Epidemiological data suggest that physical exercise is beneficial for many human diseases, including nvAMD. Yet, its protective mechanism and therapeutic potential remain unknown. Here, using clinical samples and mouse models, we found that exercise reduced CNV and enhanced anti-angiogenic therapy efficacy by inhibiting AIM2 inflammasome activation. Furthermore, transfusion of serum from exercised mice transferred the protective effects to sedentary mice. Proteomic data revealed that exercise promoted the release of adiponectin, an anti-inflammatory adipokine from adipose tissue into the circulation, which reduced ROS-mediated DNA damage and suppressed AIM2 inflammasome activation in myeloid cells of CNV eyes through AMPK-p47phox pathway. Simultaneous targeting AIM2 inflammasome product IL-1β and VEGF produced a synergistic effect for treating choroidal neovascularization. Collectively, this study highlights the therapeutic potential of an exercise-AMD axis and uncovers the AIM2 inflammasome and its product IL-1β as potential targets for treating nvAMD patients and enhancing the efficacy of anti-VEGF monotherapy.

1. Introduction

Age-related macular degeneration (AMD) is the leading cause of severe and irreversible vision loss in the elderly population in developed countries [1,2]. Specifically, neovascular AMD (nvAMD), which is characterized by the formation of choroidal neovascularization (CNV), accounts for over 80 % of the vision loss associated with AMD [3]. In this condition, abnormal blood vessels grow from the choroid and sprout into the subretinal space and neuroretina, further leading to leakage, edema, and hemorrhage, which can rapidly compromise visual function. The anti-VEGF agents, including ranibizumab, aflibercept, conbercept, and bevacizumab, are the first-line therapies for nvAMD. However,

* Correspondence to: X. Wang, Department of Pharmacology, Tianjin Key Laboratory of Inflammation Biology, The Province and Ministry Co-sponsored Collaborative Innovation Center for Medical Epigenetics, School of Basic Medical Sciences, Tianjin Medical University, Tianjin, China.
** Correspondence to: H. Yan, Department of Ophthalmology, Tianjin Medical University General Hospital, Tianjin, China.
E-mail addresses: xiaohongwang@tmu.edu.cn (X. Wang), zyyyanhua@tmu.edu.cn (H. Yan).
[1] These authors contributed equally to this work

https://doi.org/10.1016/j.metabol.2023.155584
Received 13 March 2023; Accepted 30 April 2023
Available online 5 May 2023

these therapies have limited efficacy, with only approximately 30 % of patients experience significant vision improvement. Subretinal (37.7 %), sub-retinal pigment epithelium (36.2 %), and intraretinal (61.0 %) fluid persist in many patients in long-term treatment [4,5]. Furthermore, approximately 6 %–10 % of patients demonstrated sustained visual acuity loss after intravitreal anti-VEGF therapy, mainly due to the development of foveal scars, pigmentary abnormalities, or geographic atrophy [6,7]. Therefore, it is essential to investigate alternative treatments to suppress choroid neovascularization.

Physical activity (PA) appears to protect against AMD. Beaver Dam Eye Study followed 3874 adults aged 43–86 years old for 15 years and reported that after adjusting for age, sex, and other influencing factors, active exercisers had a 70 % lower risk of nvAMD than inactive lifestyle participants, independent of body mass index (BMI) [8]. Similar findings have been reported in Caucasian populations in different countries [9]. However, the mechanism by which PA exerts beneficial effects on AMD remains unclear.

Inflammation plays a critical role in the pathogenesis and progression of AMD. Different immune cell types, inflammatory activators, and pathways are involved in AMD pathogenesis [10,11]. Choroid neovascularization is accompanied by various inflammatory cell infiltrations. Microglia and macrophages were found in human AMD lesions and are considered an important subset of immune cells [12]. Infiltration of microglia/macrophages to the sites of retinal injury can promote the growth of neovascular lesions by producing higher levels of pro-angiogenic factors such as VEGF, CCL2 and IL-8 [13,14], and experimental depletion of microglia/macrophages suppresses choroidal neovascularization in a laser-induced model [15,16]. Exercise has clear effects on the immune system [17]. However, whether and how habitual PA affects the relationship between the immune system and AMD remains to be explored. We therefore investigated how exercise affects nvAMD and the underlying mechanisms, providing translational insights into improving the efficacy of anti-angiogenic therapy.

2. Results

2.1. High-physical-activity lifestyle enhances anti-VEGF therapy efficacy in nvAMD patients

To explore whether habitual PA affects disease outcome, especially the responsiveness to anti-angiogenic therapy in nvAMD patients, we evaluated the metabolic equivalent (MET) of 25 patients with nvAMD and divided them into low PA (13 patients: 6 males and 7 females) and high PA (12 patients: 7 males and 5 females) groups. A review of patient characteristics showed no significant difference between the two groups, except that BMI was lower in the high PA group, as expected (Table S1). All 25 eyes of the 25 patients received 3+ pro re nata (PRN) anti-VEGF therapy. Optical coherence tomography (OCT) was performed before and after treatment. Retinal and lesion thicknesses showed no difference between the two groups before treatment (Fig. 1A, B). Although retinal thickness still showed no difference after three treatments, lesion thickness was significantly reduced in the high PA group compared with the low PA group, suggesting that a high PA lifestyle increased the responsiveness to anti-VEGF therapy (Fig. 1C, D).

2.2. Treadmill training protects laser-induced CNV and enhances anti-angiogenic efficacy in mice

Next, we tested whether exercise has a protective effect on CNV in mice. We employed a laser-induced photocoagulation model of CNV (laser-induced CNV model), in which laser burn of the Bruch's membrane triggers vessel growth from the choroid [18]. The mice were trained with a treadmill running regimen (six times/week; 60 min; 15 m/min) for four weeks before CNV was induced by laser photocoagulation, after which the training was stopped (Fig. 1E). Weight and blood glucose levels were monitored during the treadmill training (Tre) /sedentary (Sed) period (Fig. S1A-C). Fundus photography and OCT results showed that treadmill training did not affect the appearance and the thickness of the retina of mice without CNV (Fig. S1D-I). In CNV mice, fundus fluorescein angiography (FFA) results showed that treadmill use significantly reduced vascular leakage at days 3 and 7 after laser photocoagulation (Fig. 1F-H). The two groups did not differ significantly on day 14 (Fig. 1I), presumably due to the termination of the treadmill condition, as the body weight difference diminished seven days after the treadmill condition ended (Fig. S1C). CD31 staining of the whole-mount RPE-choroid complex also showed that treadmill use inhibited choroidal neovessel formation (Fig. 1J, K). Furthermore, OCT results showed that the thickness of CNV lesions in the Tre + CNV group was significantly lower than that in the Sed + CNV group seven days after laser photocoagulation (Fig. 1L, M). We also employed a low-intensity treadmill-running regimen (six times/week; 60 min; 12 m/min) for eight weeks, and found a comparable protective effect (Fig. S1J-N). Therefore, we performed further experiments using a four-week treadmill training regimen.

To corroborate the observation that exercise enhances the efficacy of anti-angiogenic therapy in patients, we assessed the effect of anti-angiogenic therapy in exercised or sedentary mice (Fig. 1N). Intravitreal injection of aflibercept, a soluble decoy receptor of VEGF, was protective in sedentary mice (Fig. 1O-R). Notably, when administrated to exercised mice, aflibercept showed a more robust protective effect, suggesting a synergistic effect of exercise and VEGF inhibition in the treatment of CNV (Fig. 1O-R).

2.3. Exercise exerts its protective effect via inhibition of ocular inflammation

To investigate the underlying mechanism of the observed protective effect in the treadmill group, we performed transcriptome analysis of the retina-choroid complex from sedentary or exercised mice, with or without laser coagulation. To identify the gene expression signature associated with CNV, we first compared the Sed group to the Sed + CNV group. Gene ontology (GO)-biological process (BP) analysis showed that while genes downregulated by CNV were linked to mitochondrial and visual functions; the upregulated genes were largely enriched in immune and inflammatory responses (Fig. S2A, B). This finding supports a key role of inflammatory regulation in AMD/CNV [10].

To further characterize the changes in gene expression caused by exercise in the disease situation, we compared Sed + CNV and Tre + CNV mice. We identified 2340 significantly changed genes (1382 downregulated and 958 upregulated genes) in the Tre + CNV group compared with the Sed + CNV group. GO analysis followed by network visualization of enriched GO terms using BiNGO showed that the downregulated genes were mainly associated with immune response, cell death, response to stress and stimulus, and metabolic processes (Fig. 2A), whereas the upregulated genes were mainly linked to biological regulation and development (Fig. S2C). GO-BP analysis showed that the most enriched biological process terms of the downregulated genes in the Tre-CNV group were mainly related to inflammation and immune responses (Fig. S2D). Gene set enrichment analysis (GSEA) further confirmed that genes related to inflammatory responses were significantly enriched in the Sed + CNV group, indicating that inflammation was markedly inhibited by exercise (Fig. S2E, F).

To validate these findings, we analyzed the expression of a set of inflammatory factors and adhesion molecules, including *Tnf*, *Icam1, Vcam1* and *Sele* in the retina-choroid complex of Sed + CNV and Tre + CNV mice and found that exercise suppressed these genes (Fig. S2G). GSEA also showed that macrophage activation and chemotaxis genes were significantly enriched in the Sed + CNV group (Fig. S2H, I). Moreover, compared to the Sed + CNV group, the Tre + CNV group had less macrophage infiltration in CNV lesions (Fig. 2B, C).

Next, we analyzed the signaling pathway involved in this process. Of note, the genes downregulated by exercise were significantly enriched in

the NOD-like receptor signaling pathway and the NF-κB pathway, both of which are involved in inflammasome signaling (Fig. 2D) [19,20]. Analysis of RNA-seq data from AMD patients (GSE115828) also revealed that these two signaling pathways were significantly enriched in the macula of late-phase AMD patients compared with normal macula (Fig. S2J). Treadmill training also decreased inflammasome components, including *Il1a, Il1b* and *Casp1* (Fig. S2K). Furthermore, the cleaved forms of CASP1 and IL-1β were also significantly reduced in the retina-choroid complex of Tre + CNV mice (Fig. 2E-H).

2.4. Treadmill training inhibits AIM2 inflammasome in CNV mice

To date, five receptor proteins have been confirmed to assemble inflammasomes, including NLRP1, NLRP3, NLRC4, AIM2, and Pyrin

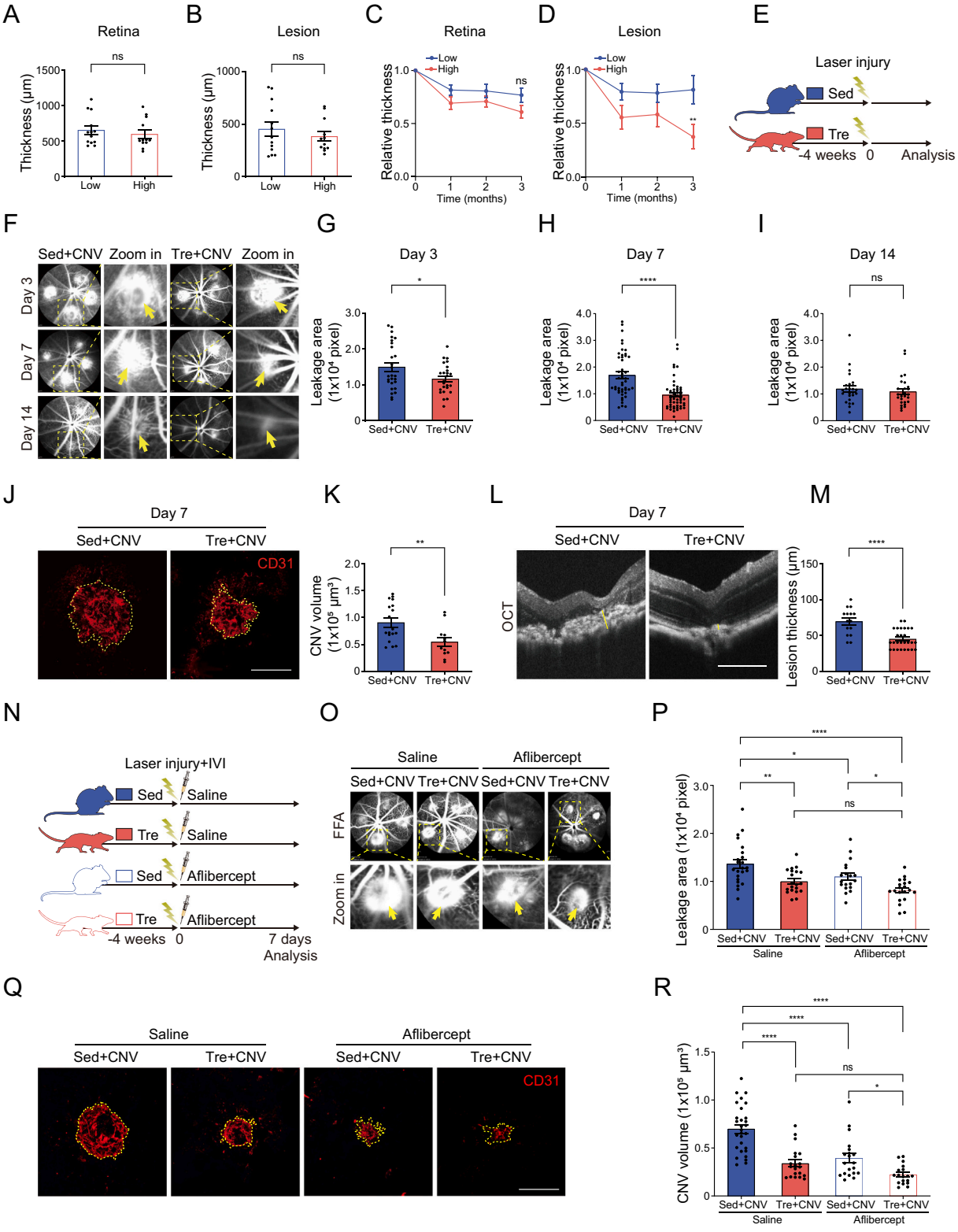

(caption on next page)

Fig. 1. Exercise inhibits CNV formation and enhances anti-angiogenic therapy efficacy in nvAMD patients and CNV model.
(A-B) Baseline (before treatment) retina (A) ($n = 13/12$ eyes from 13/12 patients) and lesion (B) (n = 13/12 eyes from 13/12 patients) thickness in patients with low PA and high PA.
(C—D) Comparison of whole retina/lesion thickness change in patients with low PA and high PA after three treatments of anti-VEGF therapy ($n = 11/10$ eyes from 11/10 patients).
(E) Schematic illustrates the chronological order of treadmill training, CNV induction, and analysis.
(F) Representative FFA images showing vascular leakage (yellow arrows) from Sed and Tre mice after laser-induced CNV at Day 3, Day 7 and Day 14.
(G-I) Quantification of the leakage area shown in (F) ($n = 27/25$ lesions from 8/4 mice per group for Day 3; $n = 46/52$ lesions from 11/8 mice per group for Day 7; $n = 25/26$ lesions from 5/8 mice per group for Day 14).
(J) Representative confocal images of CD31 stained RP*E*-choroid flat mounts from Sed + CNV and Tre + CNV mice.
(K) Quantification of the CNV volume of (J), calculated as total $CD31^+$ volume at the site of laser photocoagulation. ($n = 18/12$ lesions from 6/4 mice per group).
(L) CNV thickness in the center of laser spot were visualized using OCT. Yellow line from the lower boundary of the lesion to the higher boundary of the lesion represents the measurement range of the lesion.
(M) Quantification of lesion thickness shown in (L) ($n = 15/27$ lesions from 5/6 mice per group).
(N) Schematic illustrates the anti-VEGF therapy in Sed + CNV/Tre + CNV mice.
(O and P) FFA analysis of Sed + CNV/Tre + CNV mice treated with or without anti-VEGF therapy ($n = 23/20/19/20$ lesions from 6/5/6/7 mice per group).
(Q and R) CNV volume analysis of Sed + CNV/Tre + CNV mice treated with vehicle or Aflibercept ($n = 29/20/20/18$ lesions from 6/4/7/6 mice per group).
In all panels: $^*p < 0.05$, $^{**}p < 0.01$, $^{****}p < 0.0001$. Scale bar: 200 μm (J, L, and Q). Data represent the mean ± SEM. Values were compared using the unpaired Student's *t*-test in (A, B, G-I, K and M); one-way analysis of variance (ANOVA) multiple comparisons with Tukey's method among groups in (P and R); and two-way ANOVA with Sidak's method among groups in (C and D). IVI, intravitreal injection. (For interpretation of the references to colour in this figure legend, the reader is referred to the web version of this article.)

[21]. We found that Aim2 was most abundantly expressed in the mouse retina-choroid complex. Moreover, Aim2 was significantly induced by CNV and attenuated by treadmill training (Fig. 2I). To identify the major cell type that expresses Aim2, we analyzed an RNA-seq dataset illustrating the relative gene expression of different retinal cell types in the adult mouse retina (GSE33089) and found that *Aim2* is predominantly expressed by microglia (Fig. 2J) [22]. Because the NLRP3 inflammasome is the most well-studied receptor and responds to a diverse set of stimuli [21], we focused on both AIM2 and NLRP3.

RNA-seq results showed that both NLRP3 and AIM2 signaling were affected by treadmill training (Fig. S3A, B). Although the protein level of AIM2 was markedly decreased in the Tre + CNV group, NLRP3 level was not clearly changed (Fig. 2K, L, Fig. S3C, D). We then used *Nlrp3*$^{-/-}$ and *Aim2*$^{-/-}$ mice to investigate their role in CNV. Consistent with a previous report [23], the leakage area, CNV volume, and lesion thickness increased significantly in *Nlrp3*$^{-/-}$ mice compared to WT mice (Fig. S3E-J). However, loss of *Aim2* significantly inhibited vascular leakage, neovascularization, and lesion thickness (Fig. 2M-P, Fig. S3K, L). Collectively, these results indicate that the AIM2 inflammasome is crucial for mediating CNV progression, which in turn can be inhibited by exercise.

2.5. Serum transfusion transfers the benefits of exercise in mouse CNV model

Administration of circulating blood factors in plasma transfers the protective effect of exercise on neurogenesis and cognition [24]. To test whether blood factors also have beneficial effects in the CNV model, we harvested serum from the Sed/Tre mice 24 h after the last treadmill exercise and injected every other day into the mice without exercise. CNV was induced after two injections (Fig. 3A). FFA analysis showed a significant reduction in vascular leakage in mice administered with serum from exercised mice (Fig. 3B, C). Whole-mount staining of CD31 and Iba1 in the RPE-choroid complexes also showed that serum from the exercised mice significantly suppressed CNV formation as well as $Iba1^+$ microglia/macrophages infiltration (Fig. 3D, E). Moreover, *Icam1* and *Sele* levels in the retina-choroid complexes were significantly decreased in mice that received serum from exercised mice (Fig. 3F).

Next, we aimed to identify the circulating blood factors responsible for these protective effects. Four-dimensional (4D) label-free quantitative proteomic analysis was utilized to measure the relative amount of soluble proteins in the serum of exercised or sedentary mice. The abundance of 45 proteins increased, whereas that of 43 proteins decreased after exercise (Fig. 3G). Functional enrichment analysis using GO-BP showed that the upregulated proteins were mainly enriched in lipid metabolism, and the downregulated proteins were enriched in inflammation and complement activation (Fig. 3H, I).

2.6. Adipose tissue secreted factors in exercised mice protects against CNV

As the proteomics results of this study showed that exercised mice had lower levels of inflammatory factors in the blood circulation, we first tested whether this was responsible for the observed beneficial effects. Therefore, we analyzed serum level of IL-1β, a key inflammasome product. ELISA results showed that exercise significantly reduced IL-1β level on CNV day 3. Other inflammatory factors, such as IL-6, ICAM-1, and VCAM-1 were also reduced (Fig. S4A—D). These differences diminished on CNV day 7, presumably due to the termination of exercise after laser photocoagulation. However, in our patient cohort, the serum level of IL-1β in AMD patients in the high- and low-PA groups showed no significant difference (Fig. S4E). Pearson correlation coefficient analysis also showed no significant correlation between the lesion recovery rate and plasma IL-1β level in nvAMD patients (Fig. S4F), further suggesting that reduced IL-1β in the blood circulation might not be the cause for the protective effect. Next, we focused on the identified upregulated factors.

Using a cell types-human gene atlas database under the interactive gene list enrichment analysis platform “Enrichr”, we found that the upregulated factors were predominantly expressed in adipocytes, the placenta, and the liver (Fig. 3J). In fact, adipose tissue and the liver are the major regulatory organs that generate a range of proteins under PA, which have protective effects against multiple diseases [17,24].

To characterize the direct effects of adipose tissue and liver proteins on CNV, we used an ex vivo-choroid explant model, which is widely used to study choroidal sprouting angiogenesis [25]. Since we aimed to investigate the interaction between myeloid cells and blood vessels during CNV, we modified this model by performing laser coagulation in mice. Thus, microglia and circulating monocytes can be recruited to the lesion site [26]. The explants were then made from the choroid four days after laser injury and cultured in Matrigel (Fig. 3K). For visualization purposes, we used a *Tmem119-EGFP* mice to label $Tmem119^+$ microglia. As expected, explants from *Tmem119-EGFP* mice showed that GFP^+ microglia were present within the vessel sprouts on the choroid explants that underwent laser burn, while no GFP^+ cells were found in the choroid explant without laser (Fig. 3L). Thus, this CNV choroid explant model can be used as a myeloid cell/blood vessel interaction model to mimic the disease situation of CNV ex vivo.

We generated conditioned medium (CM) from subcutaneous adipose tissue (SAT) and liver tissue from exercised or sedentary mice (Fig. 3M, Fig. S5A). CNV choroid explants were then exposed to different CM, and their effects on choroid sprouting were analyzed. The CM of SAT from

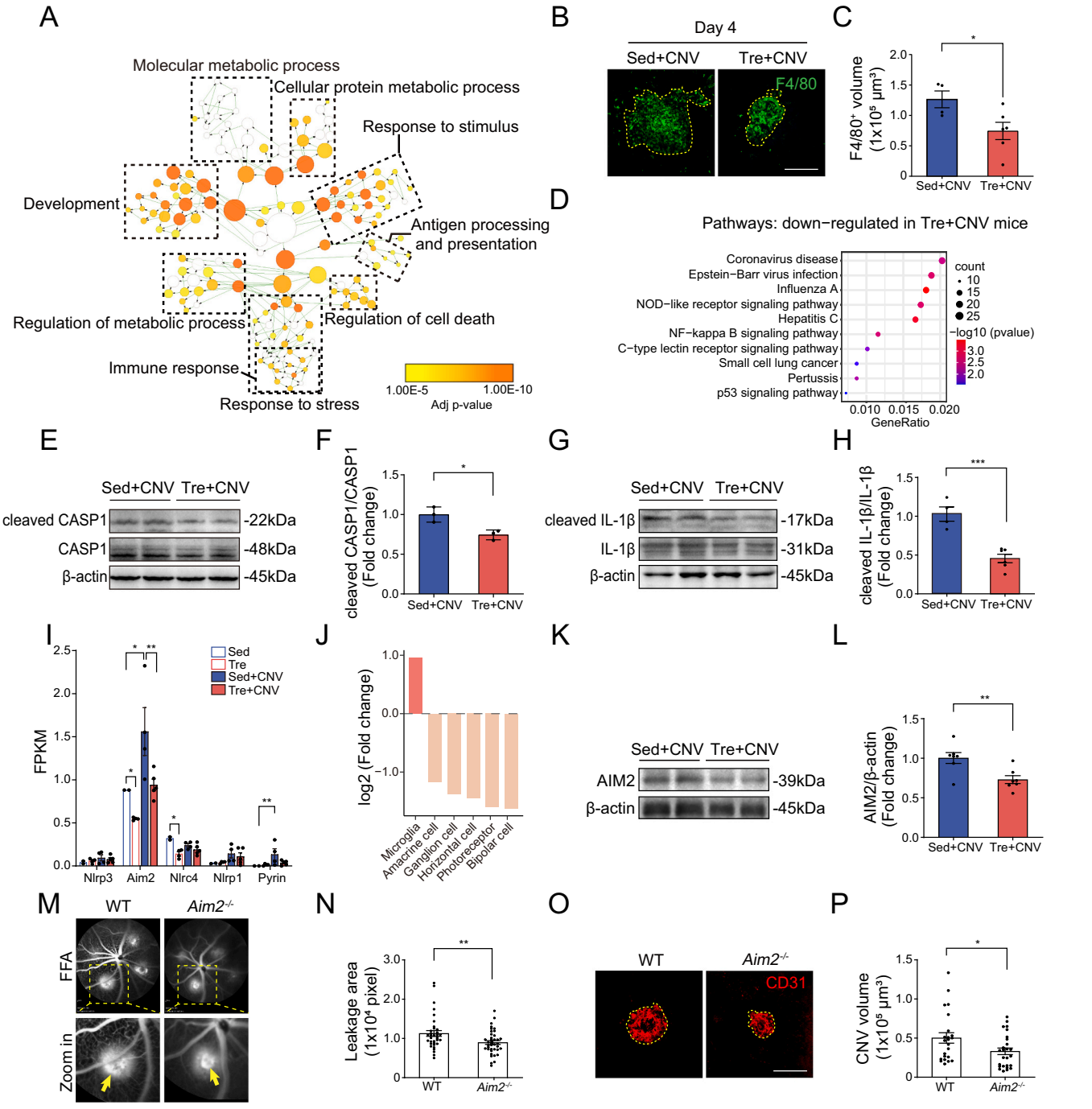

Fig. 2. Exercise suppresses inflammasome activation in CNV.

(A) RNA-seq was performed in retina-choroid complex of Sed or Tre mice four days after laser burn, BiNGO was used to visualize the GO terms network of downregulated genes in Tre + CNV compared with Sed + CNV mice.

(B) F4/80 staining of RPE-choroid flat mounts at CNV Day 4.

(C) Microglia/macrophages infiltration volumes calculated as F4/80^{+} volume surrounding the CNV lesion. (n = 4/6 lesions from 3/4 mice per group).

(D) KEGG annotation showing the enriched pathways of the significant downregulated genes in Tre + CNV vs. Sed + CNV.

(E-H) Western blotting of cleaved CASP1/CASP1 and cleaved IL-1β/IL-1β in retina-choroid complex of Sed + CNV/Tre + CNV mice four days after laser photocoagulation and quantification (n = 3/3 eyes per group for CASP1/CASP1; n = 4/6 eyes per group for cleaved IL-1β/IL-1β).

(I) The expression levels of the five inflammasome receptors analyzed from mouse retina-choroid complex RNA-seq (n = 2/4/4/5 samples per group).

(J) Expression pattern of *Aim2* in different cell types of mouse retina.

(K and L) Western blot and quantification of AIM2 expression in retina-choroid complex from Sed + CNV and Tre + CNV mice four days after laser photocoagulation (n = 7/7 eyes per group).

(M and N) FFA analysis of WT and *Aim2*$^{-/-}$ mice (n = 35/39 lesions from 8/10 mice per group).

(O and P) CNV volume analysis of WT and *Aim2*$^{-/-}$ mice (n = 23/26 lesions from 5/9 mice per group).

In all panels: *p < 0.05, **p < 0.01, ***p < 0.001. Scale bars: 200 μm (B and O). Values are presented as mean ± SEM and compared using unpaired Student's *t*-test in (C, F, H, L, N and P); Values are presented as mean ± SEM and compared by DEseq2 package in R software in (I).

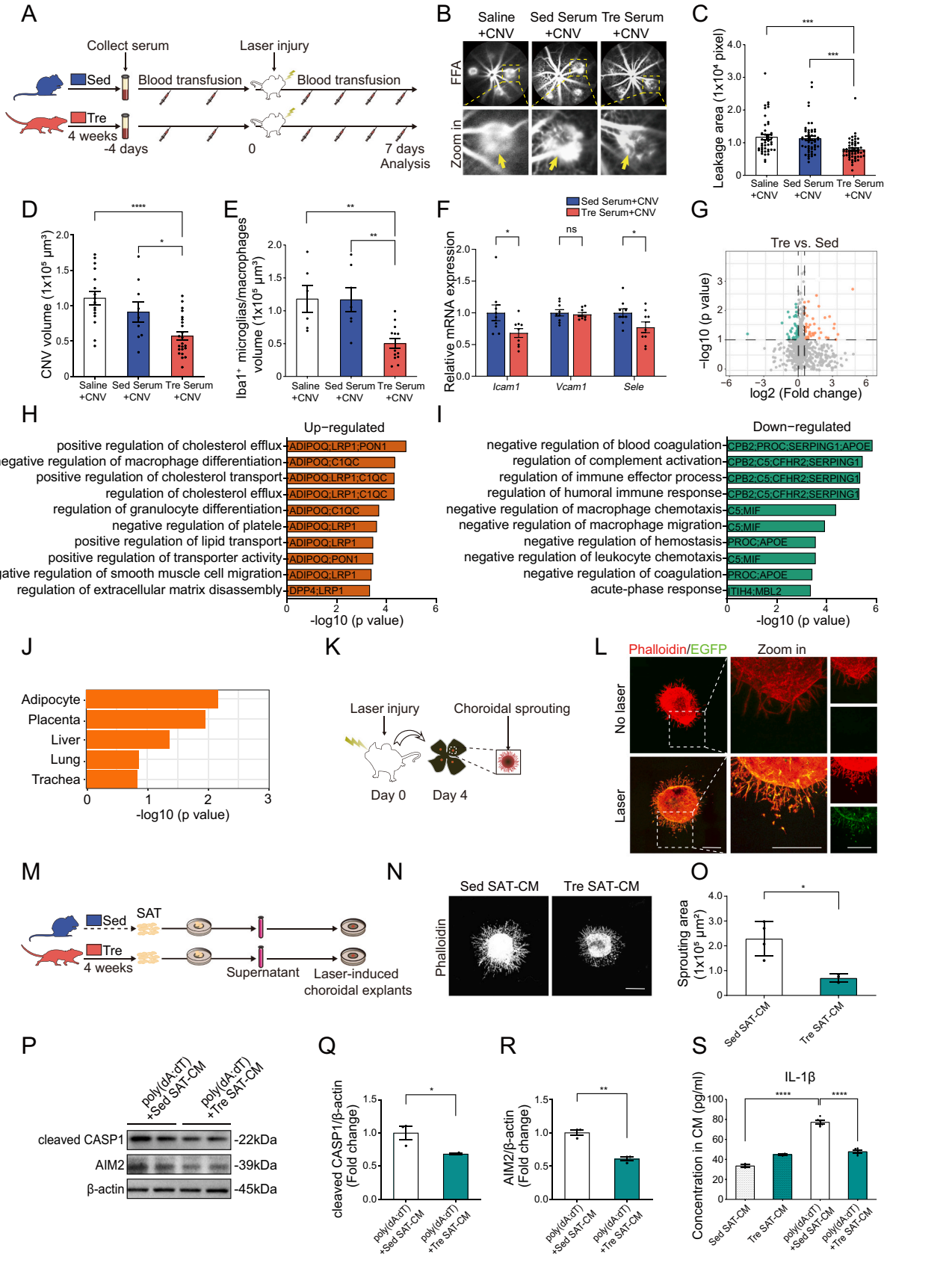

(caption on next page)

Fig. 3. Adipocyte-secreted factors in exercised mice protect CNV through blood system.
(A) Scheme of serum transfusion. Serum was collected from Sed/Tre mice and administered to age- and gender-matched sedentary mice six times over 11 days through tail vein injection (twice before laser injury).
(B and C) FFA analysis of CNV mice treated as indicated seven days after laser photocoagulation (n = 44/51/53 lesions from 11/11/11 mice per group).
(D and E) RPE-choroid flat mounts were stained for CD31 and Iba1, CNV volume (n = 17/9/23 lesions from 6/5/8 mice per group) was calculated as $CD31^+$ volume and microglia infiltration (n = 6/7/13 lesions from 3/3/6 mice per group) was calculated as $Iba1^+$ volume.
(F) qRT-PCR analysis of the expression of vascular inflammatory genes seven days after laser photocoagulation (n = 9/9 eyes per group).
(G) Serum was harvested from Sed or Tre mice for mass spectrometry analysis, volcano plot showing the distribution of detected proteins. Orange dots denote 45 proteins that are significantly upregulated by exercise and green dots denote 43 proteins significantly downregulated by exercise.
(H and I) Enrichment analysis of the serum proteins upregulated (H) and downregulated (I) by exercise, as identified by mass spectrometry.
(J) Cell type annotation of the serum proteins upregulated by exercise, as identified by mass spectrometry.
(K) Schematic illustrates a modified choroid explant model for studying myeloid cell/vascular cell interaction after CNV. RPE-choroid complex was dissected from laser-induced CNV mice and cut into 1.0 mm diameter round pieces from laser area. Then, the pieces were embedded in matrigel and cultured in M199 culture medium. The choroid sprouting could be observed after culture.
(L) Representative images showing the explant from mice with or without CNV. *Tmem119-EGFP* mice were utilized to label the microglia within the choroid explants.
(M) Schematic illustrates the preparation of SAT-CM. SAT was dissected from Sed/Tre mice and cultured in M199 endothelial growth medium; then, the SAT-CM were collected for laser-induced choroid explants.
(N) Representative images of laser-induced choroid explants exposed to SAT-CM for 48 h.
(O) Quantification of the sprouting area of (N) (n = 4/3 explants per group).
(P) BV2 were pretreated with Sed or Tre SAT-CM and then stimulated with LPS + poly(dA:dT). Western blot analysis elucidated the expression levels of cleaved CASP1 and AIM2.
(Q-R) Quantification of cleaved CASP1 (Q) (n = 3/3 biological replicates) and AIM2 (R) (n = 3/3 biological replicates).
(S) ELISA analysis of IL-1β concentration in culture medium from BV2 treated as in (P) (n = 3/3/6/6 biological replicates).
In all panels: $*p < 0.05$, $**p < 0.01$, $**** p < 0.0001$. Scale bars: 200 μm (L and N). Values as mean ± SEM. Unpaired Student's *t*-test in (F, O, Q and R); one-way ANOVA multiple comparisons with Tukey's method among groups in (C, D, E and S). (For interpretation of the references to colour in this figure legend, the reader is referred to the web version of this article.)

the exercised mice significantly suppressed choroid sprouting compared with the SAT-CM from the sedentary mice, while the liver-CM showed no difference (Fig. 3N-O, Fig. S5B, C).

Next, we tested whether SAT-CM could inhibit the activation of the AIM2-inflammasome in BV2, a mouse microglia cell line. LPS + polydA:dT is an AIM2-inflammasome activator [27]. Western blotting showed that the SAT-CM, but not the liver-CM, from exercised mice, reduced the levels of AIM2 and cleaved-CASP1 upon LPS + polydA:dT stimulation (Fig. 3P-R, Fig. S5D—F). ELISA analysis also showed that mature IL-1β was significantly suppressed by SAT-CM but not liver-CM (Fig. 3S, Fig. S5G). The above results suggested that adipose tissue, but not liver secreted factors, might be protective cues in exercised CNV mice.

2.7. Adiponectin rise upon exercise inhibits inflammasome in myeloid cells

Adiponectin, the most abundant adipokine which is known to have anti-inflammatory effects [28], was identified as an exercise-upregulating factor in our proteomic data (Fig. 3H). To validate the proteomic data, we examined adiponectin level in the serum of Sed/Tre mice 3, 7, and 14 days after training was terminated. The results showed that the adiponectin level in the Tre group was significantly higher than that in the Sed group on days 3 and 7, and the difference diminished 14 days after training (Fig. 4A). This finding is consistent with our previous data showing that the difference in CNV severity also diminished 14 days after the end of treadmill training (Fig. 1I).

We also analyzed the abundancy of adiponectin in the mice administered with serum from exercised mice compared with those administered with serum from sedentary mice, as shown in Fig. 3A. The concentration of adiponectin was higher in exercised serum-transferred recipients, suggesting that serum transfusion successfully elevated the level of adiponectin in recipient mice (Fig. 4B). Furthermore, we detected a higher level of adiponectin in the plasma of nvAMD patients with a high-PA lifestyle (Fig. 4C). Importantly, a significant correlation was found between the lesion recovery rate and plasma adiponectin level in nvAMD patients (Fig. 4D).

Next, we tested whether adiponectin was enriched in the eye after exercise. Western blotting and ELISA showed that adiponectin level were significantly higher in the retina-choroid complex, as well as in the vitreous fluid of the exercised mice (Fig. 4E-G).

Adiponectin receptor1 (AdipoR1) is the major adiponectin receptor that mediates anti-inflammatory and antioxidant roles in microglia [29]. Through analysis of single-cell RNA-seq data of the choroid in patients with AMD [30], we showed that *ADIPOR1* is predominantly expressed by microglia/macrophages, suggesting that microglia/macrophages might be the major target of adiponectin (Fig. 4H).

To evaluate the protective role of adiponectin on CNV, we treated CNV choroidal explants with vehicle or adiponectin and found that adiponectin significantly reduced choroid sprouting (Fig. 4I, J). Similarly, adiponectin suppressed AIM2, cleaved CASP1 and cleaved IL-1β in BV2 cells stimulated with LPS + polydA:dT (Fig. 4K-N). Inhibition of CASP1 activity was also observed after adiponectin treatment (Fig. 4O).

2.8. Adiponectin is essential in mediating the beneficial effects by exercise

We next wanted to determine whether adiponectin is an essential factor in mediating the protective role of exercise. To address this question, we used an $Adipoq^{-/-}$ mouse line and analyzed CNV severity after exercise.

The results showed that the leakage area and CNV volume tended to increase in sedentary $Adipoq^{-/-}$ mice compared to sedentary wild-type mice. Moreover, this difference became more pronounced in exercised mice, suggesting that adiponectin is required for the beneficial effects in exercised mice. More importantly, while in wild-type mice, treadmill training significantly reduced the leakage area and CNV volume, this protective effect was not significant in $Adipoq^{-/-}$ mice (Fig. 4P-S). These data prove that adiponectin is necessary for the protective effects of exercise.

2.9. Adiponectin suppresses AIM2 inflammasome through the inhibition of p47phox-mediated ROS production and DNA damage

Next, we aimed to elucidate how adiponectin suppresses the AIM2 inflammasome. AIM2 senses cytosolic double-stranded DNA (dsDNA) for activation, leading to the processing of IL-1β and IL-18, which are then released by pyroptosis [21]. It is known that increased ROS leads to the oxidation of DNA, and the oxidized DNA can promote DNA damage and the formation of dsDNA breaks, thereby activating the AIM2 inflammasome [27,31]. GSEA showed that ROS and DNA damage genes were significantly enriched in the Sed + CNV group (Fig. S6A, B). We also labeled ROS by CellROX and found that compared with sedentary mice, ROS accumulation in CNV lesions, especially in the $F4/80^+$ area,

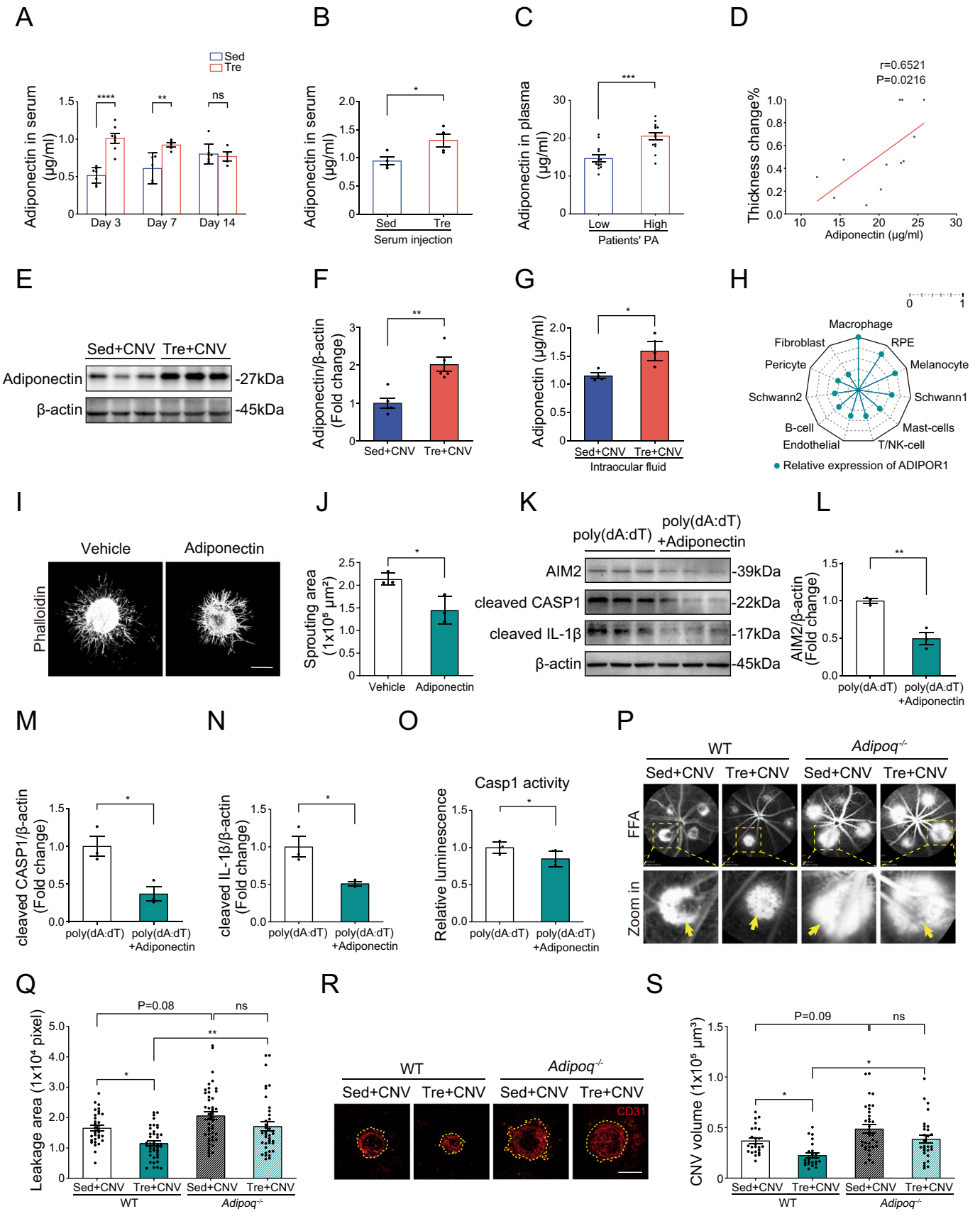

(caption on next page)

Fig. 4. Adiponectin suppresses inflammasome activation and CNV formation.
(A) ELISA analysis of serum adiponectin level at Day 3 (n = 7/7), Day 7 (n = 5/5) and Day 14 (n = 7/4) after training period was terminated.
(B) ELISA analysis of serum adiponectin level in recipient mice administrated with serum from Sed/Tre mice via the tail vein (n = 4/4).
(C) Adiponectin level in blood samples from nvAMD patients with high PA and low PA lifestyle (n = 13/14).
(D) Pearson correlation coefficient analysis of lesion recovery rate and plasma adiponectin level in nvAMD patients (n = 12). The blood sample used for analysis was obtained before anti-VEGF treatment.
(E and F) Western blot showing adiponectin expression in retina-choroid complex in Sed and Tre mice four days after laser photocoagulation (n = 5/5 eyes per group).
(G) Adiponectin level in vitreous fluid from Sed + CNV mice and Tre + CNV mice. (n = 4/3 samples per group).
(H) scRNA-seq data from retinal pigment epithelium and choroid in macular degeneration patients revealed that *ADIPOR1* is mainly expressed in macrophage in human eyes.
(I) Representative images of laser-induced choroid explants exposed to adiponectin for 48 h.
(J) Quantification of the sprouting area of (I) (n = 3/3 explants per group).
(K) Western blot of AIM2, cleaved CASP1 and cleaved IL-1β levels in BV2 pretreated with 10 μg/ml adiponectin and stimulated with LPS + poly(dA:dT).
(L-N) Quantification of AIM2 (L), cleaved CASP1 (M), and cleaved IL-1β/β-actin (N) (n = 3/3 biological replicates) shown in (K).
(O) CASP1 activity in BV2 treated as in (K) (n = 4/5 biological replicates).
(P and Q) Representative FFA images and leakage area quantification of WT and $Adipoq^{-/-}$ mice with or without treadmill training. (n = 33/43/46/38 lesions from 6/7/12/8 mice per group;).
(R and S) CNV volume analysis of WT and $Adipoq^{-/-}$ mice with or without treadmill training (n = 24/24/34/29 lesions from 6/7/11/8 mice per group).
In all panels: $^{*}p < 0.05$, $^{**}p < 0.01$, $^{***}p < 0.001$. Scale bars: 200 μm (I and R). Values are presented as mean ± SEM and compared using the unpaired Student's t-test in (A, B, C, F, G, J, L, M, N, and O); one-way ANOVA multiple comparisons with Tukey's method among groups in (Q and S).

was significantly lower in exercised mice (Fig. 5A, B). Immunofluorescence staining also showed reduced accumulation of pγH2AX-positive microglia/macrophages in the CNV lesions of exercised mice, suggesting reduced ROS-mediated oxidative DNA damage in exercised mice (Fig. 5C, D). LPS is known to increase intracellular ROS production [32]. SAT-CM from exercised mice or adiponectin treatment significantly reduced CellROX and pγH2AX level in LPS-treated BV2 cells (Fig. 5E, F, Fig. S6C—F).

Phosphorylation of p47phox is the rate-limiting step for the activation of NADPH oxidase 2 (NOX2), a key enzyme that produces ROS in microglia/macrophages [33]. The level of phospho-p47phox (pp47phox) was significantly decreased in the Tre + CNV group (Fig. 5G, H). BV2 cells treated with SAT-CM from exercised mice or adiponectin also exhibited reduced level of pp47phox upon LPS stimulation (Fig. 5I-L). AMPK, which was significantly increased upon SAT-CM from exercised mice or adiponectin treatment (Fig. 5M-P), could mediate the inhibitory effect of p47phox phosphorylation, as activated AMPK is known to be a p47phox suppressor in endothelial cells and myocardial tissue [34,35].

2.10. AAV-mediated adiponectin expression significantly alleviates CNV

To explore the therapeutic potential of adiponectin, we generated adeno-associated viruses 2 (AAV2) expressing a yellow-green fluorescent protein (AAV2-mNeonGreen) or adiponectin (AAV2-Adipoq) under the control of a constitutive CMV promoter. FFA showed that in the AAV2-mNeonGreen injected eyes, mNeonGreen expression could be detected at one week post-administration and increased during weeks 2 and 3 (Fig. 6A). Western blotting also showed that the protein level of adiponectin significantly increased in AAV2-Adipoq-administered eyes (Fig. 6B, C).

We then induced CNV three weeks after AAV2 injection (Fig. 6D). The results demonstrated that the leakage area and CNV volume were significantly decreased in mice treated with AAV2-Adipoq compared to those injected with AAV2-mNeonGreen (Fig. 6E-H).

2.11. IL1R blockade inhibits neovascularization and enhances anti-angiogenic treatment efficacy

Our observations proved that adiponectin expression using AAV2 mimics the protective effect of exercise. While AAV2-based gene therapy has emerged as a novel therapeutic modality with the potential to lead to substantial disease modification in many diseases, including ocular diseases, the duration of therapy trials is relatively long, and the cost is high. Our mechanistic study showed that adiponectin inhibited AIM2 inflammasome activation and protected against CNV progression. Thus, we wondered whether inhibition of the inflammasome product IL-1β could also be used to inhibit CNV and more importantly, to enhance the efficacy of anti-angiogenic therapy, as multiple inhibitors of IL-1β have been approved by the FDA.

To assess the effects of inhibition of the inflammasome product IL-1β, we used the IL-1 receptor (IL1R) antagonist anakinra, an FDA-approved drug for rheumatoid arthritis, cryopyrin-associated periodic syndrome, and deficiency of IL1R antagonist. By analyzing single-cell RNA-seq data of the choroid in patients with AMD [30], we found that IL1R1 was mainly expressed in endothelial cells and IL-1β was mainly expressed in macrophages in human eyes (Fig. 7A). To check whether IL-1 inhibition could also enhance the efficacy of anti-angiogenic therapy, we assessed the combined effect of anti-angiogenic therapy and anakinra. A safety test through OCT examination and TUNEL staining showed that the treatment led to no obvious toxicity in the retina (Fig. S7A-J). By analyzing vascular leakage and neovessel formation, we found that anakinra had a pronounced inhibitory effect, comparable to that of aflibercept (Fig. 7B-D). Importantly, when aflibercept and anakinra were combined, the protective effect became more robust and was significantly better than that of aflibercept or anakinra alone.

To further demonstrate the protective effect of the combination treatment, we used another mouse model. Very low-density lipoprotein receptor (VLDLR) knockout mice ($Vldlr^{-/-}$ mice) develop retinal angiomatous proliferation and choroidal neovascularization, which is similar to the neovascularization seen in macular telangiectasia and nvAMD [36]. IL-1β expression is also elevated in this model [36]. During development, growing blood vessels sprout from the deep vascular layer in the outer plexiform layer and invade the subretinal space in this model (Fig. 7E). We administered aflibercept, anakinra, or a combination of both at P11 and analyze the neovascular lesions at P18. Similar to the results of the laser-induced CNV model, while aflibercept or anakinra alone had protective effects on neovascular formation, the combination treatment achieved an even better outcome in the $Vldlr^{-/-}$ pups (Fig. 7F, G). In the adulthood of the $Vldlr^{-/-}$ mice, the ectopic vessels merged with the choroidal vessels to form retinal-choroidal anastomoses and choroidal neovascularization, the newly formed vessels are leaky which could be detected by FFA [36]. We also administered aflibercept, anakinra, or a combination in $Vldlr^{-/-}$ mice aged 6–8 weeks. FFA showed that the combination treatment relieved vascular leakage, and was significantly better than aflibercept or anakinra alone (Fig. 7H, I). Taken together, anti-angiogenic therapy combined with IL-1 inhibition significantly suppresses choroidal neovascularization, which is inspiring for the current clinical treatment of nvAMD.

3. Discussion

In this study, we characterized the protective role of physical aerobic exercise in nvAMD. Our results showed that AIM2 inflammasome activation in myeloid cells is crucial for mediating CNV progression, which could be suppressed by exercise. Moreover, we found that blood component transfusion was sufficient to impart the beneficial effects of exercise on CNV. Mechanistically, these effects are linked to adiponectin, an anti-inflammatory adipokine secreted by adipocytes. Thus, this study highlights a fat-to-eye axis through which exercise confers beneficial effects in CNV protection. Importantly, our observation that patients with a high PA lifestyle had a better outcome of anti-angiogenic therapy and that circulating level of adiponectin significantly correlated with the anti-angiogenic therapy efficacy in patients strengthened the clinical relevance of these findings.

Although inflammasomes have been implicated in mediating AMD

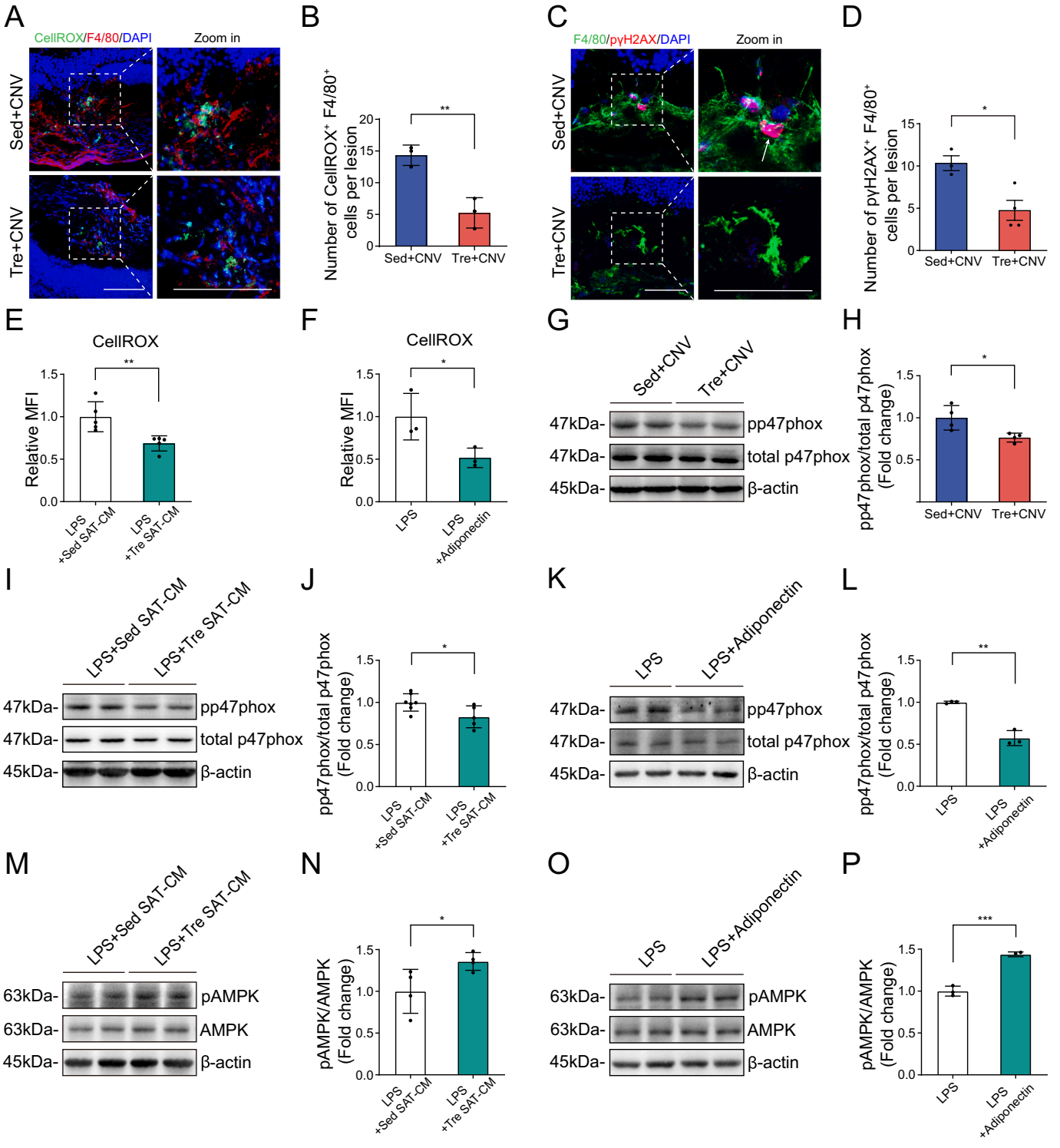

(caption on next page)

Fig. 5. Exercised SAT-CM and adiponectin suppress AIM2 activation through the inhibition of ROS production-DNA damage process via p47phox.
(A) Representative confocal images showing ROS-producing cells (CellROX, green) and microglia/macrophages (F4/80, red) in the CNV lesion.
(B) Quantification of F4/80 and CellROX-Green double positive cell number per lesion (n = 3/3 eyes per group).
(C) Immunostaining of pγH2AX and F4/80 in CNV lesions. White Arrows, pγH2AX+ nuclei.
(D) Quantification of pγH2AX and F4/80 double positive cell number per CNV lesion (n = 3/4 eyes per group).
(E) BV2 cells were pretreated with Sed or Tre SAT-CM for 12 h and then stimulated with LPS (1 μg/ml) for 6 h; CellROX was analyzed using flow cytometry (n = 5/5 biological replicates).
(F) BV2 cells were pretreated with adiponectin (10 μg/ml) for 2 h and then stimulated with LPS (1 μg/ml) for 6 h; CellROX was analyzed by flow cytometry (n = 3/3 biological replicates).
(G) Representative western blot showing pp47phox and total p47phox expression in retina-choroid complex in Sed + CNV and Tre + CNV mice four days after laser photocoagulation.
(H) Quantification of pp47phox/total p47phox (n = 5/5 eyes per group) of (G).
(I-L) Western blot showing the expression of pp47phox and total p47phox of BV2 cells treated as in (E and F) (n = 3–7/3–5 biological replicates).
(M-P) Western blot showing the expression of pAMPK/AMPK of BV2 cells treated as in (E and F) (n = 3–4/3–4 biological replicates).
In all panels: *p < 0.05, **p < 0.01, ***p < 0.001, **** p < 0.0001. Scale bar, 100 μm (A and B). Values are presented as mean ± SEM and compared using the unpaired Student's t-test in (B, D, E, F, H, J, L, N and P). MFI, mean fluorescence intensity. (For interpretation of the references to colour in this figure legend, the reader is referred to the web version of this article.)

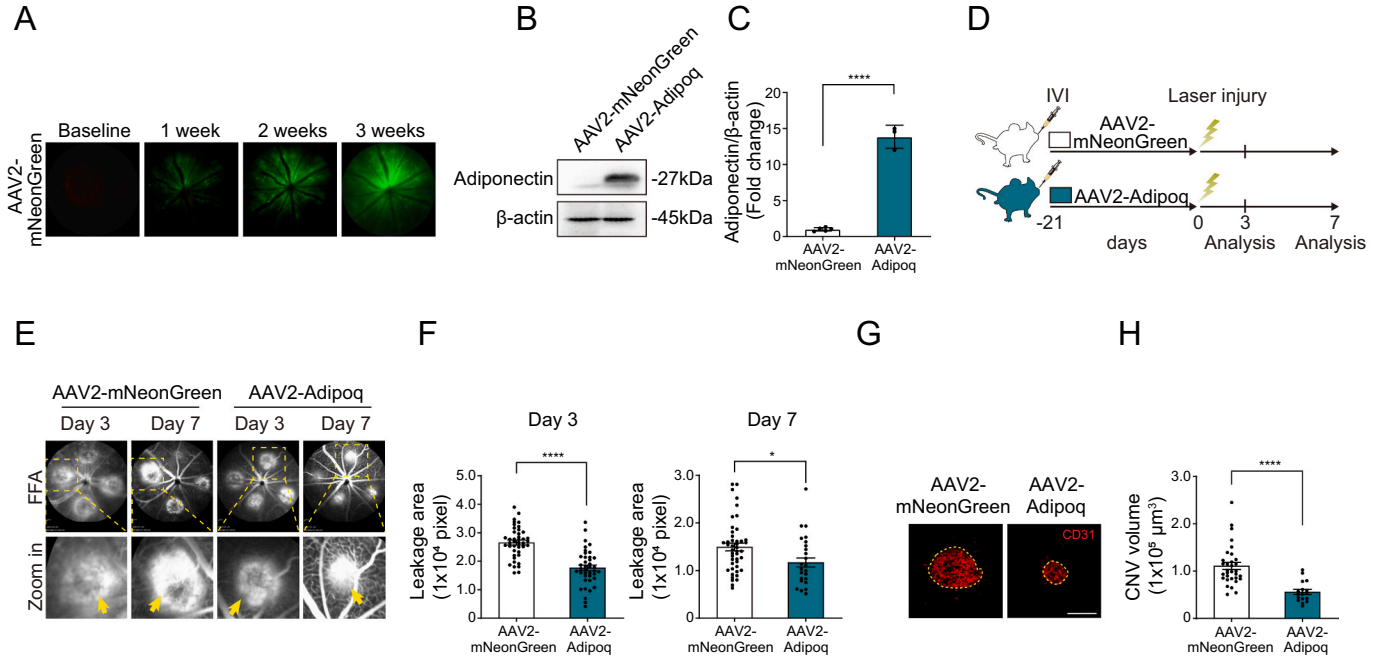

Fig. 6. Intravitreal injection of AAV2-Adipoq suppresses neovascularization in CNV model.
(A) AAV2 mediated mNeonGreen expression was determined by fundus photography at baseline before injection and 1 week, 2 weeks and 3 weeks after intravitreal injection.
(B) Western blot showing adiponectin expression in retina-choroid complex of mice three weeks after injection of AAV2-mNeonGreen/AAV2-Adipoq.
(C) Quantification of (B) (n = 3/5 eyes per group).
(D) Workflow of AAV2 intravitreal injection in CNV model.
(E) Representative images of FFA showing the vascular leakage in CNV mice pretreated with AAV2-mNeonGreen or AAV2-Adipoq.
(F) Quantification of the leakage area at Day 3 (n = 42/40 lesions from 9/7 mice per group) and Day 7 (n = 45/30 lesions from 9/6 mice per group) shown in (E).
(G) Representative confocal images of RPE-choroid flat mounts stained with CD31 in CNV mice pretreated with AAV2-mNeonGreen or AAV2-Adipoq.
(H) Quantification of the CNV volume shown in (G) (n = 32/17 lesions from 10/6 mice per group).
In all panels: *p < 0.05, **** p < 0.0001. Scale bar, 200 μm (G). Values are presented as mean ± SEM and compared using unpaired Student's t-test in (C, F, and H).

pathogenesis, their exact role is still under debate. Earlier studies mainly focused on the NLRP3 inflammasome, as NLRP3 inflammasome is activated in AMD [37–39]. However, the significance of the NLRP3 inflammasome remains unclear. While some studies have shown that blocking the NLRP3 inflammasome inhibits VEGFA-induced AMD, other studies have shown that knockout *of Nlrp3* in mice exacerbates CNV. In addition, the involvement of the non-NLRP3 inflammasome in AMD was reported recently [40,41]. Yet, the role of the AIM2 inflammasome has not been elucidated. Our RNA-seq data revealed that in the retina-RPE complex, AIM2 is the most abundant inflammasome receptor, whose expression is 21.58 ± 0.3791-fold higher than that of NLRP3 in wild-type adult mice and 16.49 ± 2.963-fold higher in laser-induced CNV mice. Our results further showed that while NLRP3 was mildly increased by CNV, which is consistent with previous studies, the induction of AIM2 was also pronounced. Using a genetic knockout model, we further demonstrated that while the absence of NLRP3 exacerbated CNV, AIM2 depletion successfully alleviated CNV. Thus, even though both NLRP3 and AIM2 inflammasomes are activated in AMD conditions, it seems that the AIM2 inflammasome predominantly promotes CNV formation, probably because of the high abundance of AIM2 in the retina-choroid complex.

IL-1β is a key product of inflammasome activation. IL-1β was also found to be highly expressed in the macular, vitreous body, and blood serum of patients with nvAMD [42–44], and it can promote vascular

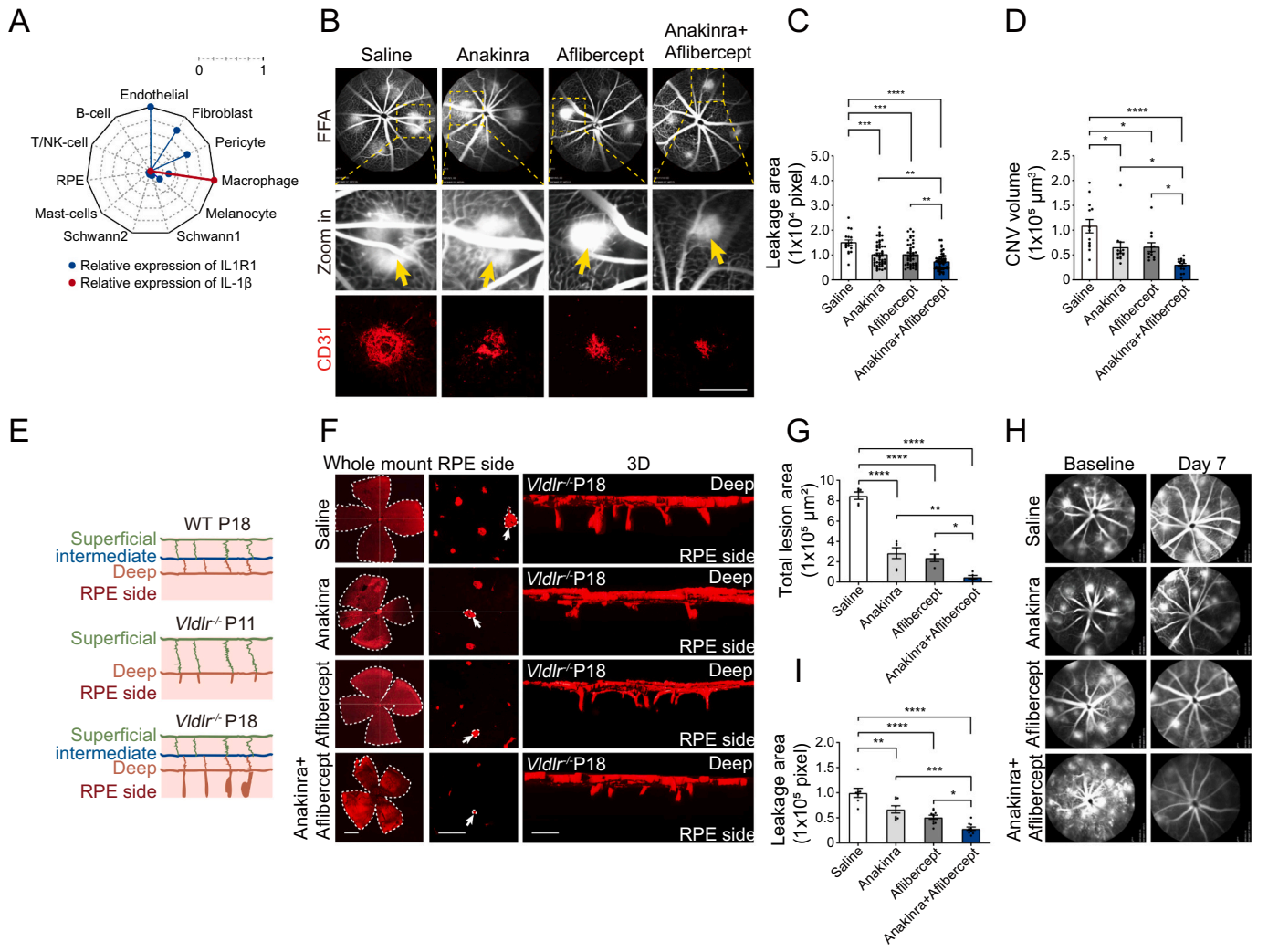

Fig. 7. IL1R blockade inhibits neovascularization in CNV model and enhances anti-angiogenic therapy efficacy.
(A) Analysis of IL1R1 and IL-1β expression from scRNA-seq data of retinal pigment epithelium and choroid in patients with macular degeneration.
(B—D) FFA and CNV volume analysis of mice with indicated treatment at CNV day 7 ($n = 17/51/47/53$ lesions from 3/10/11/13 mice per group for FFA; $n = 13/13/12/16$ lesions from 6/6/6/6 mice per group for CNV volume).
(E) Schematic illustration of normal retinal vascular development in WT mice at p18 and abnormal retinal vascular development in *Vldlr*$^{-/-}$ mice at p11 and p18.
(F) *Vldlr*$^{-/-}$ pups received the indicated intravitreal treatments at P11 and were analyzed at P18. Retinal flat mounts were stained with CD31 and representative confocal images were shown. 3D reconstruction images showing the abnormal vessel growth.
(G) Quantification of the lesion area shown in (F) ($n = 5/6/4/6$ eyes).
(H) Adult *Vldlr*$^{-/-}$ mice received the indicated intravitreal treatments and were analyzed seven days later. Representative FFA images showing the vascular leakage before (baseline) and after treatment.
(I) Quantification of the leakage area after treatment of (H) ($n = 7/8/10/10$ lesions from 4/4/5/5 mice per group).
In all panels: *p < 0.05, **$p < 0.01$, ***$p < 0.001$, **** p < 0.0001. Scale bars: 200 μm (B), 500 μm (F, whole mount), 100 μm (F, RPE side) and 50 μm (F, 3D). Values are presented as mean ± SEM and one-way ANOVA multiple comparisons with Tukey's method among groups in (C, D, G and I).

leakage and angiogenesis [45]. IL-1β is mainly produced by monocytes and macrophages and can promote the recruitment of inflammatory cells by inducing the expression of adhesion molecules on endothelial cells and chemokine secretion by stromal cells [46]. By analyzing scRNA-seq data from the choroid of nvAMD patients, we also proved that IL-1β is mainly expressed by myeloid cells (Fig. 7A) [30]. Because of the importance of IL-1 in regulating immune responses, numerous IL-1 inhibitors have been developed and applied in the treatment of multiple diseases [46,47]. Here, we used two mouse models and proved that targeting IL-1β has a safe and effective therapeutic effect on CNV, which merits further consideration in the future clinical treatment of AMD.

Anti-angiogenesis therapies targeting VEGF have a remarkable impact on neovascular ocular diseases. However, a single target of VEGF has shown limited efficacy, evoking the need to generate multitarget therapeutic strategies. To date, several bispecific reagents have been developed, such as faricimab, which targets VEGF and angiopietin2, and ABBV642, which targets VEGF and PDGFBB [48,49]. Notably, faricimab has completed phase III clinical trials to treat diabetic macular edema and nvAMD and was approved by the FDA in 2022 [50,51]. Anti-angiogenic therapy efficacy is largely dependent on the specific properties of the disease microenvironment, and understanding the features of the disease microenvironment helps generate effective therapeutic strategies [52]. Given the significant contribution of immune processes in the regulation of AMD and our result that targeting inflammatory factors, such as IL-1β, could enhance the efficacy of anti-VEGF therapy in animal models, the development of a bispecific reagent targeting VEGF and IL-1β might be beneficial in treating nvAMD patients.

The beneficial effects of PA are well recognized; however, the

mechanism is not well understood. During exercise, the sympathetic neural circuitry and neuroendocrine system coordinate adjustments in respiration, blood flow, fuel supply, and thermoregulation. Autocrine, paracrine, and endocrine factors promote crosstalk between adjacent and distant cells within or between tissues during exercise. Skeletal muscles, adipose tissue, and the liver can work as "endocrine" organs, producing and releasing proteins, metabolic intermediates, and extracellular vesicles into blood circulation, further affecting multiple physiological or pathological processes during or after exercise, such as fatty liver, cardiometabolic health, neurogenesis, and so on [24,53–55]. The anti-inflammatory effects of exercise are largely attributed to adipose tissue [56]. Although both liver- and fat-secreted factors were enriched in exercise-induced circulating factors in our study, only fat-derived CM suppressed inflammasome activation, as well as choroid spouting, further confirming the role of adipose tissue in the anti-inflammatory effects of exercise.

Adiponectin is the most abundant adipokine in the human body. Circulating adiponectin can be sequestered into injured tissue, such as atherosclerotic lesions, myocardial infarction sites, and liver injury, to prevent further damage to the surrounding tissue [57,58]. In the current study, we observed a two fold increase in adiponectin protein abundance in the eyes of exercised mice, which also supports this notion. Adiponectin exerts its actions by binding to adiponectin receptors 1 and 2. A study showed that an SNP, namely, rs10753929, located in the intron of ADIPOR1, was significantly associated with AMD in the Finnish population, providing evidence of adiponectin signaling and AMD genetic risk [59]. As our results showed that the circulating level of adiponectin significantly correlates with the efficacy of anti-angiogenic therapy in patients, it might also be valuable to consider circulating adiponectin as a biomarker that helps to predict the response of patients with nvAMD to anti-VEGF therapy.

There are three main limitations of this study. First, in this study, a self-reported questionnaire was used rather than an objective measure (such as step counting), which may have introduced recall bias. Second, this study was designed as an observational study to assess physical activity levels in patients with AMD. To fully understand whether exercise is protective in humans, studies of exercise-based interventions are desirable. Third, in our cohort of patients, we did not perform further subgroup analysis by gender due to limited sample size. It warrants further investigation on the gender dimension, as the effect of physical activity on the protection of AMD may differ by gender [60].

Taken together, using patient samples and mouse models, our findings delineate the mechanism of exercise-induced changes in the immune milieu of the eye, which provides new insights into improving the therapeutic outcome of anti-angiogenic therapies in nvAMD.

4. Material and methods

Experimental methods are described in detail in SI Materials and Methods. All patients with nvAMD were diagnosed, treated, and followed up by a single ophthalmologist (Dr. Wei Zhou) at Tianjin Medical University General Hospital from 2019 to 2022. This study was approved by the ethics committee of Tianjin Medical University General Hospital (IRB2019-WZ-101). Informed consent was obtained from all patients. All study protocols involving animal use were approved by the Institutional Animal Care and Use Committee of Tianjin Medical University (TMUaMEC 2020005).

Funding sources

This work was supported by the National Natural Science Foundation of China [grant numbers 81830026, 82020108007, 82122018, and 32171101] and the National Key R&D Program of China [2021YFC2401404].

CRediT authorship contribution statement

X. W and H. Y conceived the project, designed the study, and acquired funding. X. W, H. Y, Y. C, H. X, D. Z, and Y. Y supervised the study. B. C, K. H, X. G, W. Z, K. H, T. B, D. L, SW. Z, Y. Z, S. L, H. Z, Q. W, X. Y, Y. S, R. X, X. D, and Y. L performed the research and analyzed the data. B. C, X. W, and H. Y wrote the manuscript. All the authors reviewed the paper and approved the final draft of the manuscript.

Declaration of competing interest

Authors declare no competing interests.

Data availability

All data associated with this study are presented in the paper or Supplementary Materials.

Acknowledgments

We thank the Core Facility of Research Center of Basic Medical Sciences at Tianjin Medical University for technical support. We thank Dr. Yun Zhu (Department of Epidemiology and Biostatistics, School of Public Health Tianjin Medical University) for helpful discussions.

Appendix A. Supplementary data

Supplementary data to this article can be found online at https://doi.org/10.1016/j.metabol.2023.155584.

References

[1] Wong WL, Su X, Li X, Cheung CM, Klein R, Cheng CY, et al. Global prevalence of age-related macular degeneration and disease burden projection for 2020 and 2040: a systematic review and meta-analysis. Lancet Glob Health 2014;2:e106–16.
[2] Klein R, Klein BEK, Linton KLP. Prevalence of age-related maculopathy: the beaver dam eye study. Ophthalmology 2020;127:S122–32.
[3] Grisanti S, Tatar O. The role of vascular endothelial growth factor and other endogenous interplayers in age-related macular degeneration. Prog Retin Eye Res 2008;27:372–90.
[4] Maguire MG, Martin DF, Ying GS, Jaffe GJ, Daniel E, Grunwald JE, et al. Five-year outcomes with anti-vascular endothelial growth factor treatment of neovascular age-related macular degeneration: the comparison of age-related macular degeneration treatments trials. Ophthalmology 2016;123:1751–61.
[5] Mettu PS, Allingham MJ, Cousins SW. Incomplete response to anti-VEGF therapy in neovascular AMD: exploring disease mechanisms and therapeutic opportunities. Prog Retin Eye Res 2021;82:100906.
[6] Martin DF, Maguire MG, Fine SL, Ying GS, Jaffe GJ, Grunwald JE, et al. Ranibizumab and bevacizumab for treatment of neovascular age-related macular degeneration: two-year results. Ophthalmology 2012;119:1388–98.
[7] Ying GS, Kim BJ, Maguire MG, Huang J, Daniel E, Jaffe GJ, et al. Sustained visual acuity loss in the comparison of age-related macular degeneration treatments trials. JAMA Ophthalmol 2014;132:915–21.
[8] Knudtson MD, Klein R, Klein BE. Physical activity and the 15-year cumulative incidence of age-related macular degeneration: the beaver dam eye study. Br J Ophthalmol 2006;90:1461–3.
[9] McGuinness MB, Le J, Mitchell P, Gopinath B, Cerin E, Saksens NTM, et al. Physical activity and age-related macular degeneration: a systematic literature review and meta-analysis. Am J Ophthalmol 2017;180:29–38.
[10] Ambati J, Atkinson JP, Gelfand BD. Immunology of age-related macular degeneration. Nat Rev Immunol 2013;13:438–51.
[11] Chen M, Xu H. Parainflammation, chronic inflammation, and age-related macular degeneration. J Leukoc Biol 2015;98:713–25.
[12] McLeod DS, Bhutto I, Edwards MM, Silver RE, Seddon JM, Lutty GA. Distribution and quantification of choroidal macrophages in human eyes with age-related macular degeneration. Invest Ophthalmol Vis Sci 2016;57:5843–55.
[13] Chen M, Lechner J, Zhao J, Toth L, Hogg R, Silvestri G, et al. STAT3 activation in circulating monocytes contributes to neovascular age-related macular degeneration. Curr Mol Med 2016;16:412–23.
[14] Lechner J, Chen M, Hogg RE, Toth L, Silvestri G, Chakravarthy U, et al. Peripheral blood mononuclear cells from neovascular age-related macular degeneration patients produce higher levels of chemokines CCL2 (MCP-1) and CXCL8 (IL-8). J Neuroinflamm 2017;14:42.
[15] Espinosa-Heidmann DG, Suner IJ, Hernandez EP, Monroy D, Csaky KG, Cousins SW. Macrophage depletion diminishes lesion size and severity in

experimental choroidal neovascularization. Invest Ophthalmol Vis Sci 2003;44:3586–92.
[16] Sakurai E, Anand A, Ambati BK, van Rooijen N, Ambati J. Macrophage depletion inhibits experimental choroidal neovascularization. Invest Ophthalmol Vis Sci 2003;44:3578–85.
[17] Duggal NA, Niemiro G, Harridge SDR, Simpson RJ, Lord JM. Can physical activity ameliorate immunosenescence and thereby reduce age-related multi-morbidity? Nat Rev Immunol 2019;19:563–72.
[18] Lambert V, Lecomte J, Hansen S, Blacher S, Gonzalez ML, Struman I, et al. Laser-induced choroidal neovascularization model to study age-related macular degeneration in mice. Nat Protoc 2013;8:2197–211.
[19] Kauppinen A, Paterno JJ, Blasiak J, Salminen A, Kaarniranta K. Inflammation and its role in age-related macular degeneration. Cell Mol Life Sci 2016;73:1765–86.
[20] Marneros AG. Role of inflammasome activation in neovascular age-related macular degeneration. FEBS J 2023;290:28–36.
[21] Broz P, Dixit VM. Inflammasomes: mechanism of assembly, regulation and signalling. Nat Rev Immunol 2016;16:407–20.
[22] Siegert S, Cabuy E, Scherf BG, Kohler H, Panda S, Le YZ, et al. Transcriptional code and disease map for adult retinal cell types. Nat Neurosci 2012;15(487–95):S1–2.
[23] Doyle SL, Campbell M, Ozaki E, Salomon RG, Mori A, Kenna PF, et al. NLRP3 has a protective role in age-related macular degeneration through the induction of IL-18 by drusen components. Nat Med 2012;18:791–8.
[24] Horowitz AM, Fan X, Bieri G, Smith LK, Sanchez-Diaz CI, Schroer AB, et al. Blood factors transfer beneficial effects of exercise on neurogenesis and cognition to the aged brain. Science (New York, NY). 2020;369:167–73.
[25] Liu Z, Xu J, Ma Q, Zhang X, Yang Q, Wang L, et al. Glycolysis links reciprocal activation of myeloid cells and endothelial cells in the retinal angiogenic niche. Sci Transl Med 2020:12.
[26] Yu C, Roubeix C, Sennlaub F, Saban DR. Microglia versus monocytes: distinct roles in degenerative diseases of the retina. Trends Neurosci 2020;43:433–49.
[27] Fidler TP, Xue C, Yalcinkaya M, Hardaway B, Abramowicz S, Xiao T, et al. The AIM2 inflammasome exacerbates atherosclerosis in clonal haematopoiesis. Nature 2021;592:296–301.
[28] Choi HM, Doss HM, Kim KS. Multifaceted physiological roles of adiponectin in inflammation and diseases. Int J Mol Sci 2020;21.
[29] Jian M, Kwan JS, Bunting M, Ng RC, Chan KH. Adiponectin suppresses amyloid-beta oligomer (AbetaO)-induced inflammatory response of microglia via AdipoR1-AMPK-NF-kappaB signaling pathway. J Neuroinflamm 2019;16:110.
[30] Voigt AP, Mulfaul K, Mullin NK, Flamme-Wiese MJ, Giacalone JC, Stone EM, et al. Single-cell transcriptomics of the human retinal pigment epithelium and choroid in health and macular degeneration. Proc Natl Acad Sci U S A 2019;116:24100–7.
[31] Bird L. Taking AIM2 at atherosclerotic plaques. Nat Rev Drug Discov 2021;20:341.
[32] West AP, Brodsky IE, Rahner C, Woo DK, Erdjument-Bromage H, Tempst P, et al. TLR signalling augments macrophage bactericidal activity through mitochondrial ROS. Nature 2011;472:476–80.
[33] Roepstorff K, Rasmussen I, Sawada M, Cudre-Maroux C, Salmon P, Bokoch G, et al. Stimulus-dependent regulation of the phagocyte NADPH oxidase by a VAV1, Rac1, and PAK1 signaling axis. J Biol Chem 2008;283:7983–93.
[34] Wang S, Zhang M, Liang B, Xu J, Xie Z, Liu C, et al. AMPKalpha2 deletion causes aberrant expression and activation of NAD(P)H oxidase and consequent endothelial dysfunction in vivo: role of 26S proteasomes. Circ Res 2010;106:1117–28.
[35] Antonopoulos AS, Margaritis M, Verheule S, Recalde A, Sanna F, Herdman L, et al. Mutual regulation of epicardial adipose tissue and myocardial redox state by PPAR-gamma/Adiponectin signalling. Circ Res 2016;118:842–55.
[36] Sun Y, Lin Z, Liu CH, Gong Y, Liegl R, Fredrick TW, et al. Inflammatory signals from photoreceptor modulate pathological retinal angiogenesis via c-fos. J Exp Med 2017;214:1753–67.
[37] Tseng WA, Thein T, Kinnunen K, Lashkari K, Gregory MS, D'Amore PA, et al. NLRP3 inflammasome activation in retinal pigment epithelial cells by lysosomal destabilization: implications for age-related macular degeneration. Invest Ophthalmol Vis Sci 2013;54:110–20.
[38] Gelfand BD, Wright CB, Kim Y, Yasuma T, Yasuma R, Li S, et al. Iron toxicity in the retina requires alu RNA and the NLRP3 inflammasome. Cell Rep 2015;11:1686–93.
[39] Tarallo V, Hirano Y, Gelfand BD, Dridi S, Kerur N, Kim Y, et al. DICER1 loss and alu RNA induce age-related macular degeneration via the NLRP3 inflammasome and MyD88. Cell 2012;149:847–59.
[40] Kerur N, Fukuda S, Banerjee D, Kim Y, Fu D, Apicella I, et al. cGAS drives noncanonical-inflammasome activation in age-related macular degeneration. Nat Med 2018;24:50–61.
[41] Malsy J, Alvarado AC, Lamontagne JO, Strittmatter K, Marneros AG. Distinct effects of complement and of NLRP3- and non-NLRP3 inflammasomes for choroidal neovascularization. elife 2020:9.
[42] Nassar K, Grisanti S, Elfar E, Luke J, Luke M, Grisanti S. Serum cytokines as biomarkers for age-related macular degeneration. Graefes Arch Clin Exp Ophthalmol 2015;253:699–704.
[43] Wang Y, Hanus JW, Abu-Asab MS, Shen D, Ogilvy A, Ou J, et al. NLRP3 upregulation in retinal pigment epithelium in age-related macular degeneration. Int J Mol Sci 2016;17.
[44] Zhao M, Bai Y, Xie W, Shi X, Li F, Yang F, et al. Interleukin-1beta level is increased in vitreous of patients with neovascular age-related macular degeneration (nAMD) and polypoidal choroidal vasculopathy (PCV). PLoS One. 2015;10:e0125150.
[45] Lavalette S, Raoul W, Houssier M, Camelo S, Levy O, Calippe B, et al. Interleukin-1beta inhibition prevents choroidal neovascularization and does not exacerbate photoreceptor degeneration. Am J Pathol 2011;178:2416–23.
[46] Dinarello CA. The IL-1 family of cytokines and receptors in rheumatic diseases. Nat Rev Rheumatol 2019;15:612–32.
[47] Malcova H, Strizova Z, Milota T, Striz I, Sediva A, Cebecauerova D, et al. IL-1 inhibitors in the treatment of monogenic periodic fever syndromes: from the past to the future perspectives. Front Immunol 2020;11:619257.
[48] Ding K, Eaton L, Bowley D, Rieser M, Chang Q, Harris MC, et al. Generation and characterization of ABBV642, a dual variable domain immunoglobulin molecule (DVD-Ig) that potently neutralizes VEGF and PDGF-BB and is designed for the treatment of exudative age-related macular degeneration. MAbs 2017;9:269–84.
[49] Khan M, Aziz AA, Shafi NA, Abbas T, Khanani AM. Targeting angiopoietin in retinal vascular diseases: a literature review and summary of clinical trials involving faricimab. Cells 2020:9.
[50] Wykoff CC, Abreu F, Adamis AP, Basu K, Eichenbaum DA, Haskova Z, et al. Efficacy, durability, and safety of intravitreal faricimab with extended dosing up to every 16 weeks in patients with diabetic macular oedema (YOSEMITE and RHINE): two randomised, double-masked, phase 3 trials. Lancet 2022;399:741–55.
[51] Heier JS, Khanani AM, Quezada Ruiz C, Basu K, Ferrone PJ, Brittain C, et al. Efficacy, durability, and safety of intravitreal faricimab up to every 16 weeks for neovascular age-related macular degeneration (TENAYA and LUCERNE): two randomised, double-masked, phase 3, non-inferiority trials. Lancet 2022;399:729–40.
[52] Shen Y, Wang X, Lu J, Salfenmoser M, Wirsik NM, Schleussner N, et al. Reduction of liver metastasis stiffness improves response to bevacizumab in metastatic colorectal cancer. Cancer Cell 2020;37(800–17):e7.
[53] Kim YJ, Kim HJ, Lee SG, Kim DH, In Jang S, Go HS, et al. Aerobic exercise for eight weeks provides protective effects towards liver and cardiometabolic health and adipose tissue remodeling under metabolic stress for one week: a study in mice. Metabolism 2022;130:155178.
[54] Neufer PD, Bamman MM, Muoio DM, Bouchard C, Cooper DM, Goodpaster BH, et al. Understanding the cellular and molecular mechanisms of physical activity-induced health benefits. Cell Metab 2015;22:4–11.
[55] Zhu JY, Chen M, Mu WJ, Luo HY, Guo L. Higd1a facilitates exercise-mediated alleviation of fatty liver in diet-induced obese mice. Metabolism 2022;134:155241.
[56] Gleeson M, Bishop NC, Stensel DJ, Lindley MR, Mastana SS, Nimmo MA. The anti-inflammatory effects of exercise: mechanisms and implications for the prevention and treatment of disease. Nat Rev Immunol 2011;11:607–15.
[57] Lin Z, Wu F, Lin S, Pan X, Jin L, Lu T, et al. Adiponectin protects against acetaminophen-induced mitochondrial dysfunction and acute liver injury by promoting autophagy in mice. J Hepatol 2014;61:825–31.
[58] Denzel MS, Scimia MC, Zumstein PM, Walsh K, Ruiz-Lozano P, Ranscht B. T-cadherin is critical for adiponectin-mediated cardioprotection in mice. J Clin Invest 2010;120:4342–52.
[59] Kaarniranta K, Paananen J, Nevalainen T, Sorri I, Seitsonen S, Immonen I, et al. Adiponectin receptor 1 gene (ADIPOR1) variant is associated with advanced age-related macular degeneration in Finnish population. Neurosci Lett 2012;513:233–7.
[60] McGuinness MB, Karahalios A, Simpson JA, Guymer RH, Robman LD, Hodge AM, et al. Past physical activity and age-related macular degeneration: the Melbourne collaborative cohort study. Br J Ophthalmol 2016;100:1353–8.